Investigation of the Storage and Stability as Well as the Dissolution Rate of Novel Ilaprazole/Xylitol Cocrystal

Sihyun Nam , Changjin Lim , Yongdae Kim , Bokyoung Yoon , Taewoo Park , Woo-Sik Kim * , Ji-Hun An *

Posted Date: 4 January 2024

doi: 10.20944/preprints202401.0270.v1

Keywords: cocrystal; ilaprazole; active pharmaceutical ingredient; co-crystallization; stability; dissolution rate

Article

Investigation of the storage and stability as well as the dissolution rate of novel Ilaprazole/Xylitol Cocrystal

Sihyun Nam [1,†], Changjin Lim [2,†], Yongdae Kim [3], Bokyoung Yoon [4], Taewoo Park [4], Woo-Sik Kim [1,*] and Ji-Hun An [3,*]

[1] Functional Crystallization Center, Department of Chemical Engineering, Kyung Hee University, Yongin, Gyeonggi, 17104, Republic of Korea; skatlgus1@khu.ac.kr (S.N.)
[2] School of Pharmacy, Jeonbuk National University, Jeonju, Jeonbuk, 54896, Republic of Korea; limcj@jbnu.ac.kr (C.L.)
[3] R&D Center, UniCel Lab, Uiwang, Gyeonggi, 16079, Republic of Korea; mac8383@unicellab.com (K.Y.)
[4] R&D Center GUJU Pharm, Suwon, Gyeonggi, 16229, Republic of Korea; byyoon@guju.co.kr (B.Y.); twpark@guju.co.kr (T.P.)
* Correspondence: wskim@khu.ac.kr (W.-S.K.); wertyui12@unicellab.com (J.-H.A.)
† S. Nam and C. Lim contributed equally to this work.

Abstract: Reflux esophagitis, a treatment for gastric ulcers known as Ilaprazole (Ila), is not stable during storage and handling at room temperature, requiring storage at 5 degrees celsius. In this study, to address these issues with Ila, coformers rich in oxygen (O) and hydroxyl (OH) groups capable of forming hydrogen bonds with were selected. These coformers included Xylitol (Xyl), Meglumine (Meg), Nicotinic acid (Nic), L-Aspartic acid (Asp), and L-Glutamic acid (Glu). A 1:1 physical mixture of Ila and each coformer was prepared, and the potential for cocrystal formation was predicted using differential scanning calorimetry (DSC) screening. The results indicated the potential for cocrystal formation in the Ila/Xyl physical mixture. Subsequently, Ila and Xyl were mixed in ethyl acetate (EA) in a 1:1 ratio, and after 28 hours of slurry, the formation of Ila/Xyl cocrystal was confirmed through solid-state CP/MAS ^{13}C NMR spectrum analysis, showing intermolecular hydrogen bonding and conformational changes. Furthermore, the 1:1 ratio of Ila/Xyl cocrystal was confirmed through solution-state NMR (^{1}H, ^{13}C, and 2D) molecular structure analysis. To assess the stability of Ila/Xyl cocrystal at room temperature, it was stored and compared with Ila at 25±2°C and relative humidity (RH) of 65±5% over three months. The results showed that the purity of Ila/Xyl cocrystal remained at 99.8% from the initial purity of 99.75% over the three months, while Ila was predicted to decrease from an initial 99.8% purity to 90% after three months. Additionally, at 25±2°C and RH 65±5%, a specific impurity B in Ila/Xyl cocrystal was observed to be 0.03% over three months, whereas Ila was predicted to increase from an initial 0.032% to 2.28% after three months. To evaluate the dissolution rate of Ila/Xyl cocrystal, a formulation was prepared and compared with Ila at pH 10, with a dosage equivalent to 10mg of Ila. The results showed that Ila/Xyl cocrystal reached 55% within 15 minutes and 100% within 45 minutes, while Ila was predicted to reach 32% at 15 minutes and 100% only after 60 minutes. However, overall, the Ila/Xyl cocrystal showed results equivalent to or exceeding the dissolution rate of Ila. Therefore, it is predicted that the Ila/Xyl cocrystal will maximize its effectiveness as a more convenient crystal structure for formulation development, allowing storage and preservation at room temperature without the need for the problematic 5°C refrigeration during ambient conditions and storage, addressing the issues associated with Ila.

Keywords: cocrystal; ilaprazole; active pharmaceutical ingredient; co-crystallization; stability; dissolution rate

1. Introduction

Cocrystal refers to a form where two or more molecules form a specific stoichiometric ratio and crystal structure within a single lattice. In the context of pharmaceuticals, during the formation of cocrystals, the molecule responsible for the crystal structure, possessing activity, is referred to as the

Preprints (www.preprints.org) | NOT PEER-REVIEWED | Posted: 4 January 2024 doi:10.20944/preprints202401.0270.v1

API (Active Pharmaceutical Ingredient), while the molecule without activity is termed the coformer. Cocrystals form nonionic or noncovalent bonds, such as van der Waals forces or hydrogen bonding, within or between molecules without the need to break or induce chemical covalent bonds. Depending on the cocrystal formation, the physicochemical properties of the substance, such as solubility, dissolution rate, bioavailability, physical and chemical stability, melting point, density, etc., can change. This alteration in physicochemical characteristics offers a crystal structure that can enhance the therapeutic efficacy of the API [1-5].

Some API face challenges such as low solubility, resulting in decreased bioavailability and stability issues. To overcome these difficulties, several studies are employing co-crystallization. In the case of felodipine and xylitol, for instance, when co-crystallized in a 1:2 stoichiometric ratio, the dissolution rate increased up to 79.8% compared to felodipine alone [6]. Moreover, carbamazepine demonstrated enhanced solubility and increased absorption in the body, improving the drug's effectiveness through co-crystallization with saccharin. Drugs belonging to the propene series also experienced improved dissolution rates through co-crystallization with nicotinamide. Additionally, a drug candidate from Boehringer Ingelheim showcased superior stability characteristics through co-crystallization. In this manner, cocrystal in pharmaceutical formulations is predicted to be an effective method for enhancing solubility, bioavailability, and stability of API [7-9].

There have been recent reports on cocrystal screening using differential scanning calorimetry (DSC). This approach involves heating binary physical mixtures of the drug and coformer using a DSC device. Detailed interpretation of the obtained DSC scans can serve as a quick screening method for cocrystal detection. This is based on the assumption that the melting point of the cocrystal differs from that of the individual components. In over 50% of cases, cocrystals have demonstrated a melting point lower than both the drug and coformer [10].

Solid-state NMR (SSNMR) is an analytical technique employed to ascertain the crystal structure of materials. This method acts as a bridge between powder X-ray diffraction (PXRD) and single crystal X-ray diffraction (SXD) analytical approaches, offering insights into the conformation of the solid and the intermolecular interactions within the solid material through the chemical shifts observed in the NMR spectrum [11]. This analytical method is valuable for predicting the crystal structure of cocrystals in powder form, where obtaining a single crystal for SXD analysis is not possible. Therefore, recent research has been conducted on the interpretation of crystal structures based on intermolecular interactions in cocrystals using solid-state NMR [12-13].

Ilaprazole (Ila) (Figure 1a) is a proton pump inhibitor (PPI) used to treat gastroesophageal reflux disease and peptic ulcers, available in the market under the trade name Noltec with a 10mg dosage of Ila [14-18]. These PPI typically belong to BCS class II, presenting absorption challenges due to low aqueous solubility [19-23]. Additionally, concerns such as the emergence of specific impurities causing color changes during a 30day storage at room temperature or in solvents, resulting in a content decrease to as low as 84.2%, have been noted [17, 19, 24-25]. Despite attempts to address these stability issues through methods like salt forms [16], solvate [15], crystal form [14], and formulation change [18], satisfactory results have not been achieved.

Nevertheless, the authors of this paper, An et al., have endeavored to address this issue. They developed a 1:1 ratio Ila/Xylitol (Xyl) cocrystal with improved stability, obtaining a patent and a Chemical Abstract Service Register Number (CAS No. 2642382-31-6) [19] (Figure 1).

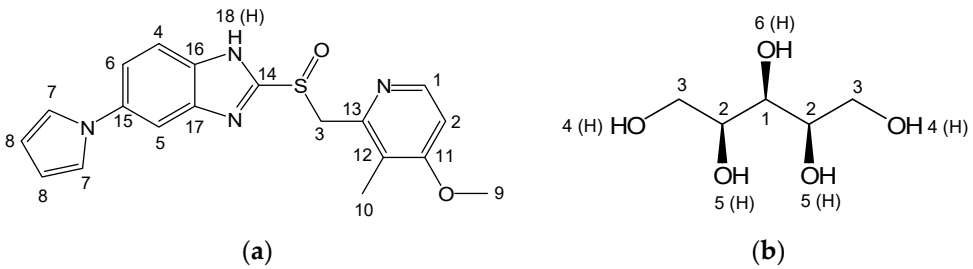

(**a**) (**b**)

Figure 1. Molecular structure with atom numbers: (a) Ilaprazole (Ila); (b) Xylitol (Xyl).

 doi:10.20944/preprints202401.0270.v1

Therefore, this paper predicts the crystal structure of the Ila/Xyl cocrystal through solid-state CP/MAS ^{13}C-NMR (SSCNMR) spectra and reports the improved stability and dissolution rate results of the Ila/Xyl cocrystal.

2. Materials and Methods

2.1. Materials

Ilaprazole (Ila) was supplied by GUJU Pharm Co. Ltd. (Korea), while Xylitol (Xyl), Meglumine (Meg), Nicotinic acid (Nic), L-Aspartic acid (Asp), and L-Glutamic acid (Glu), as well as Acetone (ACT), Methanol (MeOH), Ethanol (EtOH), and Ethyl acetate (EA), were purchased from DaeJung Chem. Co. Ltd. (Korea).

2.2. Ila/Xyl Cocrystal Preparation Using the Slurry Technique

Among the co-crystallization techniques, the slurry method involves forming cocrystals through solvent-mediated phase transformation (SMPT) of a mixture of API and coformer [1, 26]. Therefore, it is more convenient for cocrystal production compared to the grinding method and proves to be efficient for large-scale production. In this study, the researchers employed the slurry technique to enhance the ease of production and preparation of Ila/Xyl cocrystals. The experimental procedure involved adding 10g of Ila and 4.2g of Xyl (1 equivalent (1eq.)) to a 300mL reactor, followed by the addition of 100mL of EA. The mixture was stirred at 200rpm for 36 hours, resulting in the formation of a 1:1 ratio Ila/Xyl cocrystal.

2.3. Differential Scanning Calorimetry (DSC)

For cocrystal screening of Ila and characterization analysis of Ila/Xyl cocrystals using DSC, a TA Instruments DSC Q20 (TA Instruments, Philadelphia, PA, USA) with Tzero pan and Lid (TA Instruments, Philadelphia, PA, USA) was utilized. The thermal profile was analyzed in a nitrogen atmosphere from 30 ℃ to 350 ℃ at a scan rate of 10 ℃/min.

2.4. Thermogravimetric Analysis (TGA)

To perform thermogravimetric analysis of Ila/Xyl cocrystals, a TGA Q50 (TA Instruments, Philadelphia, PA, USA) was used in a nitrogen atmosphere. The temperature range was set from 30 ℃ to 400 ℃, and the scan rate was 10 ℃/min.

2.5. Powder X-ray diffraction (PXRD)

Ila/Xyl cocrystal forms was analyzed with a Powder X-ray diffractometer (Bruker, D8 Advance, Billerica, Massachusetts, USA) equipped with Cu Ka radiation set at 45kV and 40mA. The divergence and scattering slits were set as 1°, and the receiving slit was 0.2mm. The 2θ scanning range was from 5° to 35° with a scanning rate of 3°/min (0.4 sec/0.02°).

2.6. Solution-State Nuclear Magnetic Resonance Spectroscopy (Solution-State NMR)

For molecular structure determination, confirmation of the Ila and Xyl ratio, and atomic numbering of Ila, Xyl, and Ila/Xyl cocrystals, 1D (^{1}H, ^{13}C) and 2D (COSY, HSQC, HMBC) solution-state NMR spectra were obtained using a BRUKER AVANCE-800 (Billerica, MA, USA). Ila, Xyl, and Ila/Xyl cocrystals were dissolved in DMSO-d^{6} for NMR analysis.

2.7. Solid-State Nuclear Magnetic Resonance Spectroscopy (Solid-State CP/MAS ^{13}C-NMR(SSCNMR))

The solid-state CP/MAS ^{13}C-NMR spectra of Ila, Xyl and Ila/Xyl cocrystal were recorded with a 500 MHz solid-state NMR (Avance II, Bruker, Billerica, MA, USA). The spectral acquisition was achieved using the cross polarization (CP)/magic angle spinning (MAS) pulse sequence.

Preprints (www.preprints.org) | NOT PEER-REVIEWED | Posted: 4 January 2024 doi:10.20944/preprints202401.0270.v1

Experimental condition was as follows: spinning 5 KHz; pulse delay, 10 s; contact time, 2 min; analysis time, 24 h.

2.8. Stability Test at 25 ± 2 °C and Relative Humidity (RH) 60±5%

To assess the stability of Ila/Xyl cocrystal and Ila during storage and preservation, a stability chamber (T&H chamber, Jeio Tech, Daejeon, Korea) was utilized. The samples were stored under conditions of 25±2°C and relative humidity (RH) of 60±5% for a duration of 3 months. The changes in purity were observed using high-performance liquid chromatography (HPLC) with a Waters 2487 instrument (Milford MA, USA). Additionally, the formation of a specific impurity, ilaprazole sulfur ether (impurity B) (Figure 2), was monitored [17]. The analysis was performed using a C18 column (4.6 × 150 mm, 5 μm, Kromasil®, Bohus, Sweden). Mobile phase A consisted of 0.01 mol/L ammonium hydrogen phosphate (pH 6.8)/acetonitrile/methanol 90:5:5 (v/v/v), while mobile phase B comprised 0.01 mol/L ammonium hydrogen phosphate (pH 6.8)/acetonitrile/methanol 40:30:30 (v/v/v). The flow rate was set at 1.5 mL/min, wavelength at 237 nm, and run time at 50 min. Ila and impurity standards were obtained from GUJU Pharm Co. Ltd. (Korea). A 10 mg standard solution was prepared by dissolving 1.32 g of ammonium hydrogen phosphate in 750 mL of purified water, adjusting the pH to 11.5 with a 1 mol sodium hydroxide solution. The samples were prepared by injecting 40 mL of the solution, and the retention times of Ila and impurity were confirmed. The results showed that Ila appeared at 15.7 min, and ilaprazole sulfur ether (impurity B) at 21.1 min (Figures S1-S2). The stability chamber samples of Ila/Xyl cocrystal and Ila were prepared using the same method as the standard samples (stored at 5°C during measurements, as Ila is unstable when dissolved in the solvent, and stability was confirmed for 24 hours under 5°C storage conditions [17].)

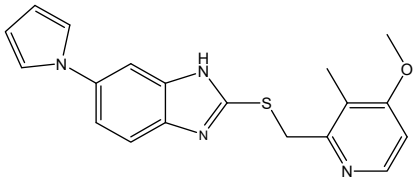

Figure 2. Molecular structure of ilaprazole sulfur ether (impurity B) [Ref.17].

2.9. Variable-Temperature Powder X-ray Diffraction (VT-PXRD)

To confirm the melting temperature (Tm) of the Ila/Xyl cocrystal in the DSC thermal profile, a Powder X-ray diffractometer (Bruker, D8 Advance, Billerica, Massachusetts, USA) with an added hot stage accessory was employed. VT-PXRD analysis was conducted at temperatures of 25°C, 55°C, 95°C, and 105°C, using the same conditions as in the PXRD analysis outlined in section 2.5. This allowed for the verification of the Tm of the Ila/Xyl cocrystal.

2.10. Comparison of Dissolution Rates between Formulated Ila/Xyl Cocrystal and Ila

To compare the dissolution rates of Ila/Xyl cocrystal and Ila, formulations were obtained from GUJU Pharm Co. Ltd. (Korea), including the formulated product Noltec for Ila (Ila dosage: 10mg) and the Ila/Xyl cocrystal formulation (Ila dosage: 10mg) (Figure 3). Subsequently, dissolution testing was conducted using the Dissolution Apparatus (Agilent 708-DS, Santa Clara, CA, USA) with the USP dissolution testing apparatus II Paddle (37 °C ± 0.5 °C). Dissolution tests were performed using a dissolution test solution consisting of a pH 10 buffer solution (4L) mixed with 0.5% Polysorbate 80. Samples were collected at 0, 5, 10, 15, 30, 45, and 60-minute intervals, and high-performance liquid chromatography (HPLC) (Waters 2487, Milford MA, USA) was employed for analysis. The dissolution analysis conditions included the use of a C18 column (4.5 × 75 mm, 5 μm, Kromasil®, Bohus, Sweden), with the mobile phase prepared by mixing dissolution test buffer solution (3.4g potassium dihydrogen phosphate and 0.9g sodium hydroxide dissolved in 600mL purified water) and acetonitrile in a 65:35 (v/v) ratio. The pH was adjusted to 8.3 using a 1 mol sodium hydroxide solution. The flow rate was set at 1.5 mL/min, wavelength at 237nm, and run time at 50 min. To

 doi:10.20944/preprints202401.0270.v1

determine the peak area of Ila, a 10mg Ila standard was dissolved in 100mL of dissolution test buffer. This standard solution was then diluted 100 times with the dissolution test buffer, and the peak area of Ila was confirmed using this diluted standard solution. The dissolution rate was calculated using the formula: (Peak area of Ila from the sample / Peak area of Ila from the diluted standard solution) × (Amount of Ila standard collected (10mg) / 10) × (900/1000) × purity of the standard (%) (The dissolution analysis method and calculation followed the standards and testing methods of the Ila formulation product name Noltec (Ila dose: 10mg) as specified by the Korean Food and Drug Administration (KFDA)).

(**a**) (**b**)

Figure 3. Formulation images of Ila and Ila-Xyl cocrystal: (a) Ila formulation (brand name: Noltec (10 mg as Ila)); (b) Ila/Xyl cocrystal (10 mg as Ila).

3. Result and Discussion

3.1. Cocrystal Screening of Ila Using DSC

The possibility of screening the formation of cocrystals through the heating of API (Active Pharmaceutical Ingredient) and coformer physical mixtures using DSC (Differential Scanning Calorimetry) has been reported. This is attributed to the different melting points of the API, coformer, and cocrystal [10]. Therefore, in this study, to address issues related to the poor stability and release rate during the storage and handling processes of Ila, we aimed to develop cocrystals of Ila with enhanced stability. For this purpose, five potential coformers rich in functional groups such as OH and O, capable of forming hydrogen bonds with Ila (pKa 10.10 [27]), were selected, as presented in Table 1 and Figure S3 [13].

Table 1. Hydroxy group used as coformer and their pKa.

Coformer (equivalent)	pKa (Ref. [28])
L-Aspartic acid (Asp) (1eq.)	1.88
	3.65
L-Glutamic acid (Glu) (1eq.)	2.19
	4.25
Meglumine (Meg) (1eq.)	9.52
Nicotinic acid (Nic) (1eq.)	4.85
Xylitol (Xyl) (1eq.)	12.76

After preparing physical mixtures of the coformers and Ila in a 1:1 ratio, as indicated in Table 1 and Figure S3, DSC screening was conducted, and the results are presented in Figure 4. In Figure 4 (a) and (b), the DSC thermal profiles of the Ila/Asp and Ila/Glu physical mixtures did not show any new exothermic or endothermic peaks; instead, the profiles exhibited a mixed form. Therefore, Asp and Glu were predicted to have no potential for cocrystal formation with Ila and were excluded.

In Figure 4 (c), the DSC thermal profile of the Ila/Meg physical mixture showed an endothermic peak around 128°C and a new exothermic peak around 150°C. The endothermic peak at 130°C appeared slightly ahead of the endothermic peak of Meg at 130°C, and the endothermic peak

Preprints (www.preprints.org) | NOT PEER-REVIEWED | Posted: 4 January 2024 doi:10.20944/preprints202401.0270.v1

corresponding to Ila at 162°C was absent. In Figure 4 (d), the DSC thermal profile of the Ila/Nic physical mixture did not exhibit predicted endothermic and exothermic peaks associated with Ila and Nic. Instead, a new endothermic peak appeared at approximately 138°C, and a new exothermic peak emerged at around 147°C. The presence of new endothermic and exothermic peaks in the DSC thermal profiles of physical mixtures indicates the potential for cocrystal formation. This is because the formation of exothermic peaks in the DSC thermal profiles can predict phase transformation into a cocrystal, and changes in endothermic peaks can be indicative of variations in the melting point [10].

Lastly, in Figure 4 (e), the DSC thermal profile of the Ila/Xyl physical mixture exhibited a matched endothermic peak of Xyl at 98°C. However, new small endothermic and exothermic peaks appeared at 147°C and 153°C, respectively. Furthermore, the endothermic peak corresponding to Ila at 162°C was not observed. These results suggest the potential for new interactions or changes in the melting point, providing insight into the possibility of cocrystal formation [10].

Thus, with the predicted potential for cocrystal formation through DSC screening, co-crystallization attempts were made using Meg, Nic, and Xyl via the co-crystallization technique known as slurry.

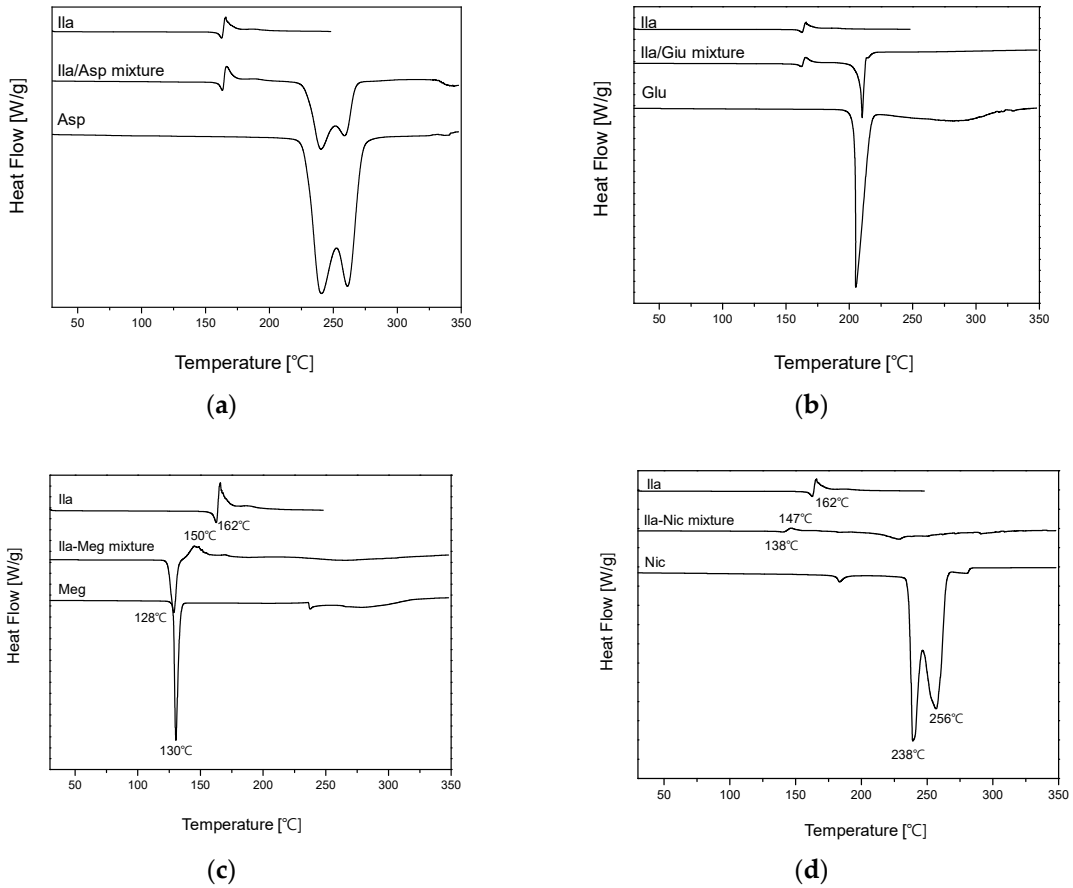

Preprints (www.preprints.org) | NOT PEER-REVIEWED | Posted: 4 January 2024 doi:10.20944/preprints202401.0270.v1

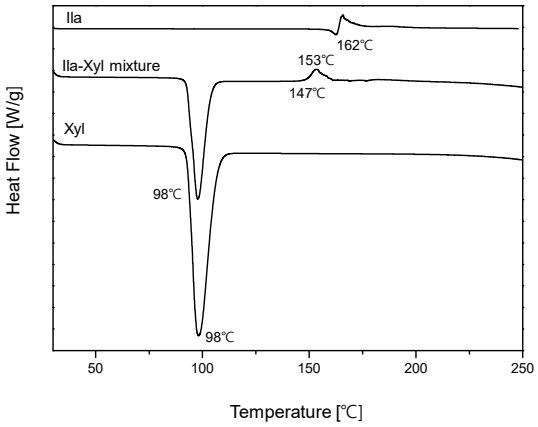

(**e**)

Figure 4. Ila cocrystal screening using DSC: (a) Ila, Asp and Ila/Asp (1:1) physical mixture; (b) Ila, Glu and Ila/Glu (1:1) physical mixture; (c) Ila, Meg and Ila/Glu (1:1) physical mixture; (d) Ila, Nic and Ila/Nic (1:1) physical mixture; (e) Ila, Xyl and Ila/Xyl (1:1) physical mixture**.**

3.2. Co-Crystallization of Ila Using the Slurry Technique

Based on the DSC thermal profile results in Figure 4, coformers Meg, Nic, and Xyl, which showed potential for cocrystal formation with Ila, were selected. Ila (1g) and the chosen coformer (1eq.) were individually added to MeOH, ACT, EtOH, and EA solvents (10mL each) and stirred at room temperature for 24 hours to assess the potential for co-crystallization. In MeOH, ACT, and EtOH solvents, either Ila or the coformer dissolved, making it impossible to obtain a solid or obtaining only a small amount. Therefore, these solvents were excluded. However, in EA, a significant amount of solid was obtained. EA was chosen as the solvent, and Ila (10g) was used, stirring at room temperature for 36 hours, followed by PXRD analysis.

The results indicated that both Ila/Meg and Ila/Nic exhibited PXRD patterns similar to the physical mixture, suggesting no potential for co-crystal formation (Figures S4-S5). However, for Ila/Xyl, the PXRD pattern differed significantly from the PXRD patterns of Ila, Xyl, and the physical mixture.

Figure 5 shows the PXRD patterns of Ila, Xyl, Ila/Xyl physical mixture, and the Ila/Xyl obtained through co-crystallization. In the PXRD pattern of the co-crystallized Ila/Xyl, peaks at 2θ were observed at 6.83°, 12.57°, 15.78°, 18.06°, 19.42°, 19.74°, and 22.46°. In contrast, the 2θ values for the Ila/Xyl physical mixture were 7.34°, 13.02°, 16.15°, 18.55°, 22.84°, 25.82°, and 31.81°. Additionally, Xyl exhibited peaks at 2θ values of 14.85°, 17.91°, 22.84°, and 24.96°, while Ila showed peaks at 2θ values of 7.29°, 13.02°, 16.20°, 18.50°, 21.50°, and 25.84°. Therefore, it is predicted that the Ila/Xyl crystal obtained through co-crystallization has a new crystal structure, indicating the potential for cocrystal formation. However, further analysis is needed for a conclusive result.

Preprints (www.preprints.org) | NOT PEER-REVIEWED | Posted: 4 January 2024 doi:10.20944/preprints202401.0270.v1

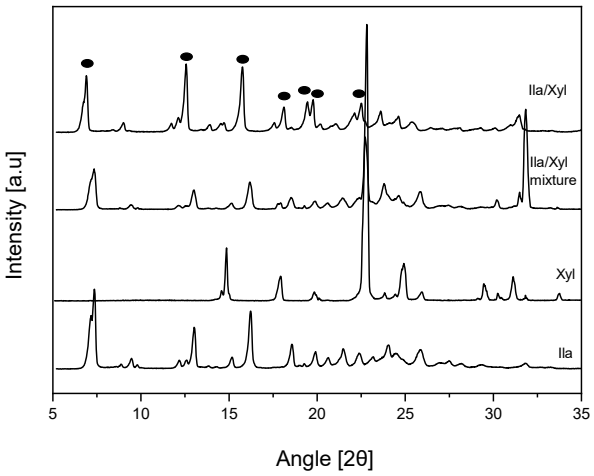

Figure 5. PXRD pattern of Ila, Xyl, Ila/Xyl physical mixture and Ila/Xyl crystal obtained by co-crystallization.

3.3. Prediction of Intermolecular Interaction in Ila/Xyl Cocrystal Using Solid-state CP/MAS 13C-NMR (SSCNMR)

To predict that the Ila/Xyl crystal obtained through co-crystallization is indeed a cocrystal, attempts were made to analyze it using SSCNMR. To interpret the analyzed SSCNMR spectra, solution-state NMR 1D (1H, 13C) and 2D (1H-1H COSY, 1H-13C HSQC, 1H-13C HMBC) were analyzed. The molecular structures of Ila, Xyl, and Ila/Xyl were interpreted, and the positions of carbon (C) and hydrogen (H) were confirmed by numbering them according to the molecular structures of Ila and Xyl, as seen in Figure 1. This information served as the basis for interpreting the SSCNMR spectrum analysis (Figure S6 - Figure S20).

Figure 6 presents the SSCNMR spectra of Ila, Xyl, Ila/Xyl physical mixture, and the Ila/Xyl crystal obtained through co-crystallization. As observed in the SSCNMR spectra of Figure 6, it can be predicted that the spectrum of the Ila/Xyl crystal obtained through co-crystallization shows differences in chemical shift and split of peaks compared to the spectra of Ila, Xyl, and the Ila/Xyl physical mixture.

Preprints (www.preprints.org) | NOT PEER-REVIEWED | Posted: 4 January 2024 doi:10.20944/preprints202401.0270.v1

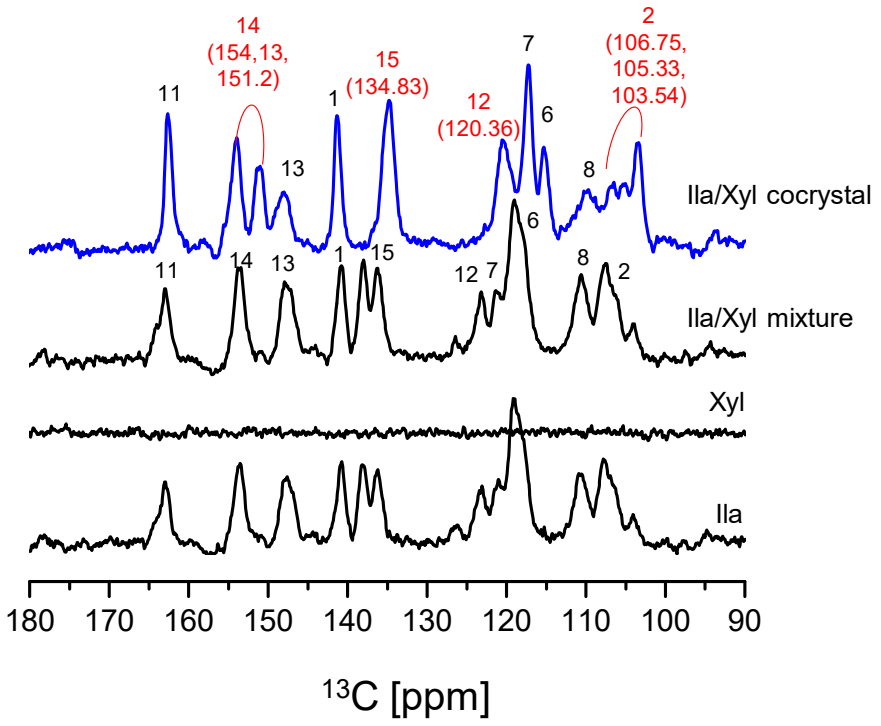

(**a**)

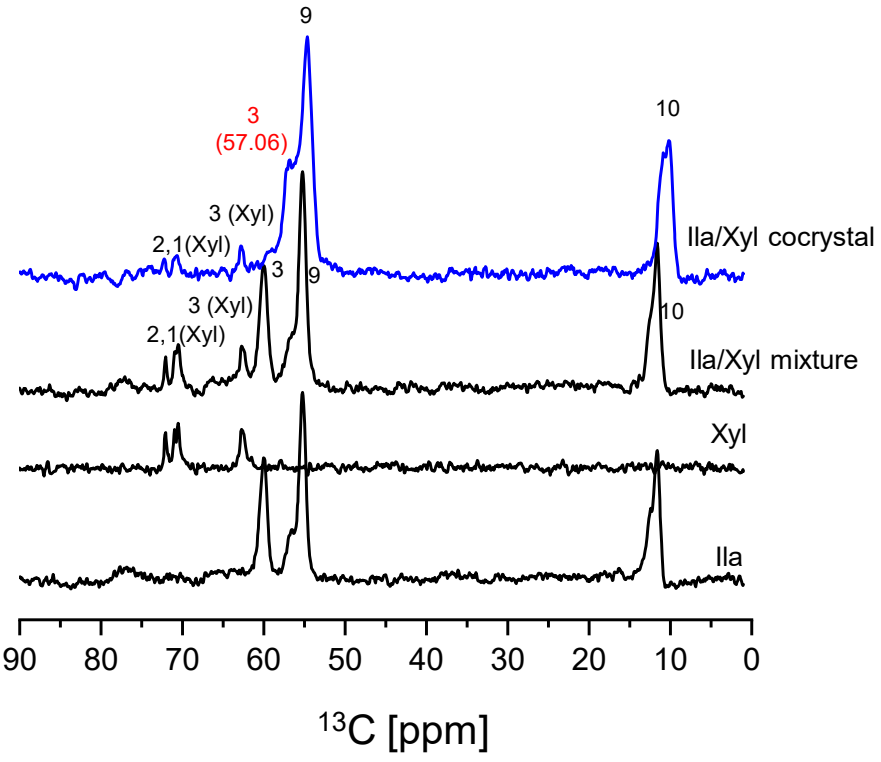

(**b**)

Figure 6. Ila/Xyl (1:1) cocrystal, Ila, Xyl, and Ila/Xyl (1:1) physical mixture's solid-state CP/MAS 13C-NMR: (a) 90-180ppm; (b) 0ppm-90ppm (Numbers on the peaks are related to numbers in Figure 1 structure location).

 doi:10.20944/preprints202401.0270.v1

In Figure 6 (a), when comparing the spectrum of the Ila/Xyl crystal obtained through co-crystallization (shown in blue) with the spectra of Ila, Xyl, and the Ila/Xyl (1:1) physical mixture, a noticeable shift in C15 to a more upfield position at 134.83 ppm can be observed from the Ila molecular structure in Figure 1 (a). This shift is predicted to result from the benzimidazole N-H(18) in the Ila structure acting as a hydrogen bond donor. The enhanced electron density due to acting as a hydrogen bond donor would affect the resonance of C15 at the para position, causing it to shift upfield.

Furthermore, in Figure 6 (a) of the Ila/Xyl crystal obtained through co-crystallization, changes in the split of C14 are observed at 154.13 ppm and 151.2 ppm. This change is anticipated to be influenced by the benzimidazole N-H(18) in the Ila structure acting as a hydrogen bond donor and the sulfoxide S=O acting as a hydrogen bond acceptor, as indicated in Figure 1 (a). Evidence supporting the sulfoxide S=O as a hydrogen bond acceptor can be inferred from the changes in the chemical shift of C3 in Figure 6 (b).

Additionally, significant changes in the chemical shifts of C2 and C12 in Figure 6 (a) are predicted to be due to the nitrogen (N) of the pyridine in the Ila structure acting as a hydrogen bond acceptor, leading to changes in the chemical shift of C2 and C12 through resonance effects.

In Figure 6 (b), the SSCNMR spectrum shows Xyl C1, C2, and C3 appearing in the range of 60 ppm to 75 ppm, as indicated in Figure 1 (b). However, it is observed in this spectrum that there is no significant difference in chemical shift and split. This lack of difference is attributed to molecular structures with hydroxy groups (OH), such as Xyl, being capable of acting as both hydrogen bond acceptors and donors simultaneously. Therefore, such molecular structures can exhibit both intramolecular and intermolecular interactions, resulting in a consistent electron distribution. As a consequence, the SSCNMR spectrum in Figure 6 (b) is predicted to show no significant differences in chemical shift and split due to these interactions [29].

The results of the SSCNMR spectrum in Figure 6 predict the presence of hydrogen bonds, specifically between the N-H (donor) of Ila and the O (acceptor) of Xyl, the S=O (acceptor) of Ila and the O-H (donor) of Xyl, as well as the N (acceptor) of Ila and the O-H (donor) of Xyl..

SSCNMR is an effective tool for predicting intermolecular interactions and conformational changes through changes in chemical shift and splitting. It becomes particularly valuable when single crystals cannot be precipitated, and SXD analysis is not feasible for predicting crystal structures [11-13]. Therefore, based on the SSCNMR results in Figure 6, it is predicted that the Ila/Xyl crystal obtained through co-crystallization can be identified as a cocrystal. The reason Ila and Xyl could form a cocrystal in a slurry, i.e., a solvent, is attributed to the small acidity difference between Ila and Xyl as indicated in Table 1. The low acidity prevents ionization between the two molecules in the solvent environment, and the abundance of functional groups capable of forming intermolecular interactions further supports this prediction

Furthermore, the formation of Ila/Xyl cocrystal in a 1:1 ratio was predicted through solution-state ^{1}H-NMR spectra (Figure 7). This result was further refined and confirmed through ^{1}H-NMR analysis (Figure S16) and 2D ^{1}H-^{1}H COSY analysis (Figure S18).

Preprints (www.preprints.org) | NOT PEER-REVIEWED | Posted: 4 January 2024 doi:10.20944/preprints202401.0270.v1

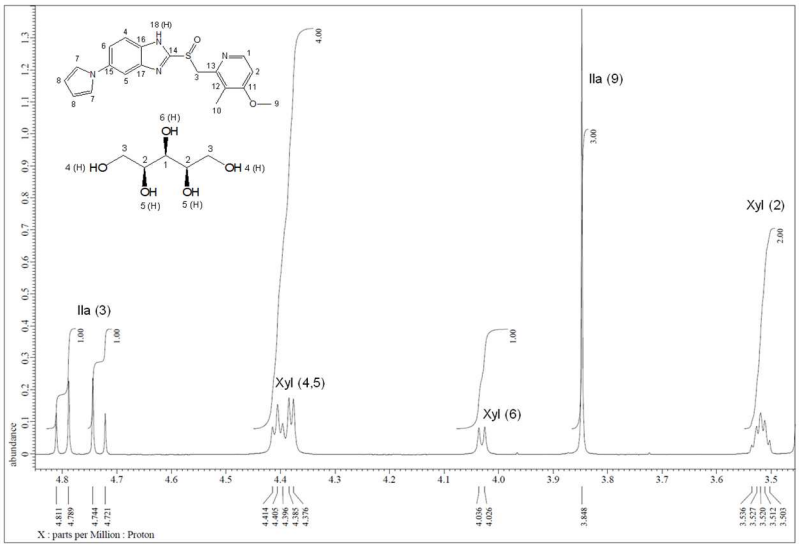

Figure 7. Integration of solution-state ^{1}H-NMR spectrum of IIa/Xyl cocrystal (DMSO-d^{6}).

3.4. Thermal Analysis of IIa/Xyl Cocrystal

Figure 8 shows the DSC (Differential Scanning Calorimetry) heat curves and TGA (Thermogravimetric Analysis) results for IIa/Xyl cocrystal, IIa, and Xyl. In the results, the IIa/Xyl cocrystal exhibits an endothermic peak at 93.62°C, while IIa shows an endothermic peak at 162.48°C, and Xyl at 98.17°C. Additionally, in TGA, the IIa/Xyl cocrystal starts to experience mass loss due to thermal decomposition around 140°C, IIa at 155°C, and Xyl at approximately 220°C.

Despite the fact that there isn't a significant difference in the endothermic temperatures between IIa/Xyl cocrystal and Xyl, to precisely determine the melting temperature, VT-PXRD analysis was conducted to predict its accuracy.

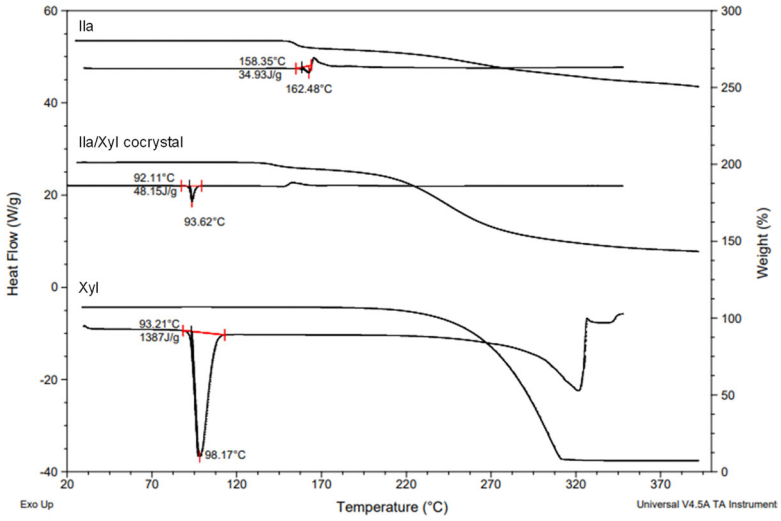

Figure 8. TGA-DSC curves of IIa/Xyl cocrystal, IIa and Xyl (heating rate 10°C/min).

Figure 9 shows the VT-PXRD (Variable Temperature Powder X-ray Diffraction) patterns of IIa/Xyl cocrystal analyzed in the temperature range from 25°C to 105°C. This analysis was conducted to predict that the DSC endothermic peak observed at 93.62°C in Figure 8 corresponds to the melting temperature.

In the results, at 25°C and 55°C, the PXRD patterns maintain the same 2θ values, indicating the stability of the cocrystal. However, at 95°C, which corresponds to the endothermic temperature observed in Figure 8, the PXRD pattern is nearly disappearing. Furthermore, at 105°C, no distinct

Preprints (www.preprints.org) | NOT PEER-REVIEWED | Posted: 4 January 2024 doi:10.20944/preprints202401.0270.v1

peaks related to 2θ are observed, indicating the complete absence of the characteristic PXRD pattern. This suggests that from 95°C onward, the Ila/Xyl cocrystal melts, and the PXRD pattern is not evident. Therefore, the temperature of the DSC endothermic peak in Figure 8, representing the Ila/Xyl cocrystal, can be predicted as the melting temperature by observing the VT-PXRD pattern changes.

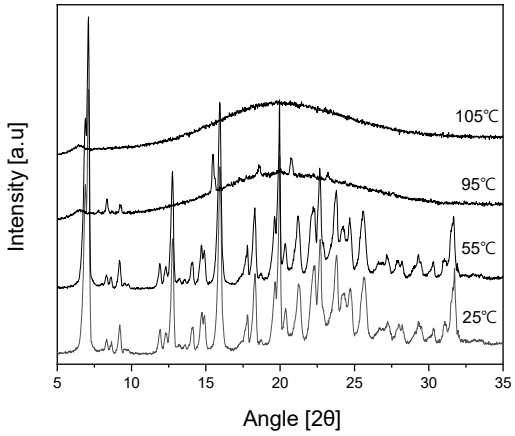

Figure 9. VT-PXRD pattern of Ila/Xyl cocrystal according to temperature change**.**

The analysis results from Tables 1-2 and Figures 5-9 predict the formation of a 1:1 ratio cocrystal between Ila and Xyl, and the characterization of this cocrystal has been confirmed.

3.5. Stability Evaluation for Room Temperature Storage at 25±2°C and RH 65±5% of Ila/Xyl Cocrystal

Proton pump inhibitors (PPIs) such as Ila often face challenges in stability, with issues like discoloration and the generation of specific impurities, such as ilaprazole sulfur ether (impurity B in Figure 2), during storage at room temperature for 30 days. This results in a decrease in purity to below 95%, posing problems for its use as an active pharmaceutical ingredient (API) and formulation development. Consequently, storing Ila at 5°C has been reported to the Korea Ministry of Food and Drug Safety (KMFDS) [17, 19, 24-25].

APIs with low stability present difficulties in formulation development, product handling, dosage form issues, and analytical method challenges. Cocrystals, as crystalline solids formed by the intermolecular interaction between an API and a coformer, can share the advantages of the coformer with the API. Consequently, they offer a promising solution to overcome the current issues with Ila, providing an optimal crystal structure that enhances stability, solubility, and dissolution rates [1-5].

Figure 10 depicts the results of stability testing conducted by the researchers to predict whether the newly developed Ila/Xyl cocrystal improves the low stability associated with Ila during room temperature storage. Ila and Ila/Xyl cocrystal were subjected to stability chambers under conditions of 25±2°C and RH 65±5% for three months, and their purity was assessed. As observed in Figure 10, the Ila/Xyl cocrystal maintains its high purity, with minimal changes, from an initial purity of 99.8% to 99.8% after one month and 99.75% after three months. In contrast, Ila shows a decline in purity from an initial 99.8% to 94% after one month and further to 90% after three months, highlighting the improved stability of the cocrystal compared to Ila alone.

Preprints (www.preprints.org) | NOT PEER-REVIEWED | Posted: 4 January 2024 doi:10.20944/preprints202401.0270.v1

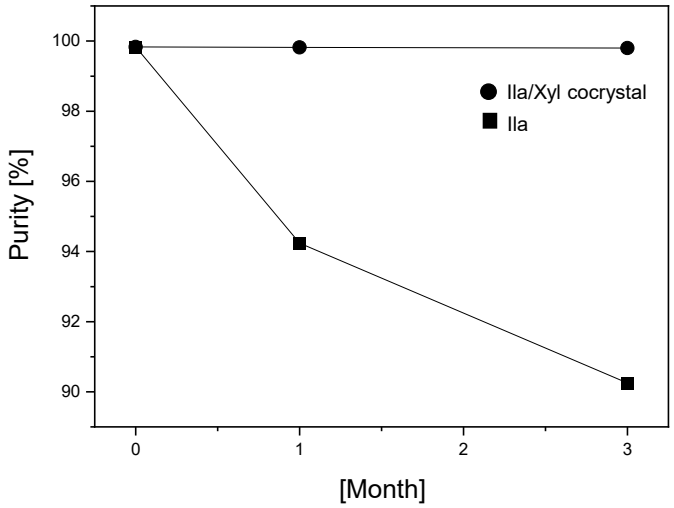

Figure 10. Purity Results Analyzed After 3 Months of Storage at 25±2°C and RH 65±5% for Ila and Ila/Xyl Cocrystal**.**

Table 2 presents the results of HPLC analysis to determine whether a specific impurity, ilaprazole sulfur ether (impurity B, Figure 2 [17]), was generated in the samples over the 3-month period. The analysis was conducted by confirming the retention time of ilaprazole sulfur ether using HPLC (Figure S1).

Table 2. Results of ilaprazole sulfur ether impurity analysis after 3 months of storage at 25±2°C and RH 65±5% for Ila and Ila/Xyl cocrystal.

Month	Ila	Ila/Xyl cocrystal
0	0.032%	0.004%
1	0.82%	0.023%
3	2.28%	0.030%

As shown in Table 2, the Ila/Xyl cocrystal exhibited minimal generation of the impurity ilaprazole sulfur ether (Figure 2) over the storage period. The initial content was 0.004%, increasing to 0.023% after 1 month and 0.030% after 3 months, remaining well below 0.1%. In contrast, Ila showed a significant increase in a specific impurity, ilaprazole sulfur ether, starting from an initial content of 0.032% to 0.82% after 1 month and further to 2.28% after 3 months.

Molecules with structures like Xyl can engage in both intramolecular and intermolecular interactions, acting as both hydrogen bond acceptors and donors. This property contributes to the overall stability of the molecule [29-30]. The improved stability of Ila through cocrystallization with Xyl, as observed in Figure 10 and Table 2, is attributed to the intermolecular interaction with Xyl as a coformer, leading to the formation of the cocrystal.

Therefore, it is predicted that the Ila/Xyl cocrystal, with its enhanced stability, can be stored and maintained at room temperature. The cocrystal demonstrates the potential for Ila to serve as an improved solid-state form with enhanced stability as an active pharmaceutical ingredient (API).

3.6. Comparison of Dissolution Rates between Ila/Xyl Cocrystal Formulation and Ila Noltec Formulation

Ila is commercially available under the product name Noltec at a dosage of 10mg. However, due to the expiration of the patent, efforts have been made to launch Ila as a generic drug by developing

Preprints (www.preprints.org) | NOT PEER-REVIEWED | Posted: 4 January 2024 doi:10.20944/preprints202401.0270.v1

salt forms [16], solvates [15], crystal forms [14], and formulation changes [18] to achieve an equivalent or higher dissolution rate. Despite these efforts, generic market entry has proven challenging.

Figure 11 illustrates the dissolution rate results for the Ila/Xyl cocrystal formulated at a dosage of 10mg (as shown in Figure 3) and the Ila Noltec formulation (dosage: 10mg). In this graph, the Ila/Xyl cocrystal reaches 54.33% at 15 minutes, 96.49% at 30 minutes, and 100% at 45 minutes. In comparison, Ila achieves 33.67% at 15 minutes, 94.45% at 30 minutes, 98.15% at 45 minutes, and 100% at 60 minutes. Although the dissolution rate of the Ila/Xyl cocrystal may be slightly faster than that of Ila, considering the margin of error, it is predicted to be roughly equivalent. Despite not achieving an equivalent or higher dissolution rate, the Ila Noltec formulation has faced challenges in the generic drug market. However, the Ila/Xyl cocrystal, with the advantage of stable storage at room temperature, is expected to expedite the generic drug launch process.

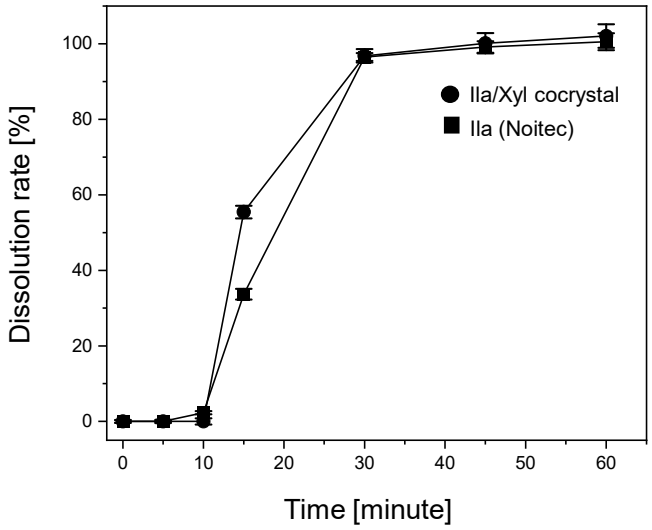

Figure 11. Dissolution Rate Test at pH 10 for Ila/Xyl Cocrystal Formulation (Dosage: 10mg) and Ila Noltec Formulation (Dosage: 10mg) (Refer to the Formulation Images in Figure 3).

4. Conclusions

In this study, we aimed to address the stability issues of Ila, a medication used for the treatment of gastroesophageal reflux disease (GERD) and peptic ulcers, marketed under the brand name Noltec (10 mg). The challenge was to improve its stability at room temperature and during storage. As a result, we successfully formed a cocrystal of Ila and Xyl in a 1:1 ratio, which can be stored at room temperature without the need for refrigeration. The predicted crystal structure of the Ila/Xyl cocrystal was confirmed through the analysis of solid-state cross-polarization/magic angle spinning carbon-13 nuclear magnetic resonance (SSCNMR) spectra, providing insights into the intermolecular interactions between Ila and Xyl.

The enhanced stability of the Ila/Xyl cocrystal was demonstrated through a three-month stability evaluation under conditions of 25±2°C and relative humidity (RH) 65±5%. The cocrystal maintained a purity of 99.8% throughout the storage period, whereas the purity of Ila decreased to 90% after three months, accompanied by the significant generation of a specific impurity, ilaprazole sulfur ether. The improved stability of the Ila/Xyl cocrystal was attributed to the inherent stability of the coformer Xyl, suggesting that the intermolecular interactions between Ila and Xyl played a crucial role.

Furthermore, dissolution rate tests comparing the Ila/Xyl cocrystal formulation (10 mg) and the commercial Ila formulation Noltec (10 mg) were conducted at pH 10. The results indicated that the Ila/Xyl cocrystal exhibited a dissolution rate comparable to or slightly faster than that of Ila Noltec. This suggests that the cocrystal formulation, with its enhanced stability and potential for room

temperature storage, could expedite the generic drug release process for Ila, addressing the challenges faced by the generic pharmaceutical industry in developing equivalent dissolution rates.

In conclusion, the development of the Ila/Xyl cocrystal not only overcomes the stability issues associated with Ila, allowing for room temperature storage, but also offers advantages in formulation development, product handling, dosing, and analytical testing. The cocrystal, with its improved stability and dissolution characteristics, represents an optimal crystalline structure, providing a promising solution for the challenges associated with Ila as an active pharmaceutical ingredient (API). Therefore, the development of cocrystals is anticipated to play a crucial role in future pharmaceutical development, not only for enhancing absorption rates in drugs with solubility issues but also for improving the physicochemical properties of APIs through the unique characteristics of crystal structures.

Supplementary Materials: The following supporting information can be downloaded at: www.mdpi.com/xxx/s1, Figure S1. Shows the chromatogram of Ilaprazole (Ila) impurity obtained through High-performance liquid chromatography (HPLC) analysis, depicting the retention time (RT). (RT: 21.062min); Figure S2. Shows the chromatogram of Ilaprazole (Ila) obtained through High-performance liquid chromatography (HPLC) analysis, depicting the retention time (RT). (RT: 15.689min); Figure S3. The molecular structures of the coformers presented in Table 1; Figure S4. PXRD pattern of Ila, Meg, Ila/Meg physical mixture and Ila/Meg obtained by co-crystallization; Figure S5. PXRD pattern of Ila, Nic, Ila/Nic physical mixture and Ila/Nic obtained by co-crystallization; Figure S6. Solution-state ^{1}H-NMR of Ilaprazole (Ila) (solvent: DMSO-d^{6}) (Hydrogen numbering for each peak has been completed.); Figure S7. Solution-state ^{13}C-NMR of Ilaprazole (Ila) (solvent: DMSO-d^{6}) (Carbon numbering for each peak has been completed.); Figure S8. Solution-state 2D NMR (^{1}H-^{1}H COSY) of Ilaprazole (Ila); Figure S9. Solution-state 2D NMR (^{1}H-^{13}C HSQC) of Ilaprazole (Ila); Figure S10. Solution-state 2D NMR (^{1}H-^{13}C HMBC) of Ilaprazole (Ila); Figure S11. Solution-state ^{1}H-NMR of Xylitol (Xyl) (solvent: DMSO-d^{6}) (Hydrogen numbering for each peak has been completed.); Figure S12. Solution-state ^{13}C-NMR of Xylitol (Xyl) (solvent: DMSO-d^{6}) (Hydrogen numbering for each peak has been completed.); Figure S13. Solution-state 2D NMR (^{1}H-^{1}H COSY) of Xylitol (Xyl); Figure S14. Solution-state 2D NMR (^{1}H-^{13}C HSQC) of Xylitol (Xyl); Figure S15. Solution-state 2D NMR (^{1}H-^{13}C HMBC) of Xylitol (Xyl); Figure S16. Solution-state ^{1}H-NMR of Ila/Xyl cocrystal (solvent: DMSO-d^{6}); Figure S17. Solution-state ^{13}C-NMR of Ila/Xyl cocrystal (solvent: DMSO-d^{6}); Figure S18. Solution-state 2D NMR (^{1}H-^{1}H COSY) of Ila/Xyl cocrystal; Figure S19. Solution-state 2D NMR (^{1}H-^{13}C HSQC) of Ila/Xyl cocrystal; Figure S20. Solution-state 2D NMR (^{1}H-^{13}C HMBC) of Ila/Xyl cocrystal.

Author Contributions: Conceptualization, W.-S.K. and J.-H.A.; methodology, C.L., S.N., B.Y.,T.P., K.Y. and J.-H.A.; investigation, C.L., S.N., B.Y.,T.P., K.Y. and J.-H.A.; visualization, S.N. B.Y.,T.P., and J.-H.A.; writing—original draft preparation, C.L., S.N. and J.-H.A.; writing—review and editing, C.L., S.N., B.Y.,T.P., K.Y., W.-S.K. and J.-H.A.; All authors have read and agreed to the published version of the manuscript.

Data Availability Statement: Not applicable.

Conflicts of Interest: The authors declare no conflict of interest.

References

1. Sathisaran. I.; Dalvi. S.V. Engineering Cocrystals of Poorly Water-Soluble Drugs to Enhance Dissolution in Aqueous Medium. *Pharmaceutics*. **2018**, 10, 108.
2. Nanjwade, V. K.; Manvi, F. V.; Nanjwade, B. K.; Maste, M. M. New trends in the co-crystallization of active pharmaceutical ingredients. *Journal of Applied Pharmaceutical Science*. **2011**, 08, 01-05.
3. Alvani, A.; Shayanfar, A. Solution Stability of Pharmaceutical Cocrystals. *Cryst. Growth Des.* **2022,** 22(10), 6323-6337.

4. Steed. J.W. The role of co-crystals in pharmaceutical design. *Trends in Pharmacological Sciences.* **2013**, 34(3), 185-193.
5. Sugden, I. J.; Braun, D. E.; Bowskill, D. H.; Adjiman, C. S.; Pantelides, C. C. Efficient Screening of Coformers for Active Pharmaceutical Ingredient Cocrystallization. *Cryst. Growth Des.* **2022**, 22(7), 4513-4527.
6. Arafa, M. F.; El-Gizawy, S. A.; Osman, M. A.; El Maghraby, G. M. Xylitol as a potential co-crystal co-former for enhancing dissolution rate of felodipine: preparation and evaluation of sublingual tablets. *Pharmaceutical development and technology.* **2018**, 23(5), 454-463.
7. Tomaszewska, I. In vitro and Physiologically Based Pharmacokinetic models for pharmaceutical cocrystals. Doctoral dissertation, University of Bath. Doctoral dissertation, University of Bath. 31 Dec 2013, (https://researchportal.bath.ac.uk/en/studentTheses/in-vitro-and-physiologically-based-pharmacokinetic-modelsfor-phar).
8. Chow, S. F.; Chen, M.; Shi, L.; Chow, A. H.; Sun, C. C. Simultaneously improving the mechanical properties, dissolution performance, and hygroscopicity of ibuprofen and flurbiprofen by cocrystallization with nicotinamide. *Pharmaceutical research,* **2012**, 29, 1854-1865.
9. Kim, S.; Li, Z.; Tseng, Y. C.; Nar, H.; Spinelli, E.; Varsolona, R.; Senanayake, C. Development and characterization of a cocrystal as a viable solid form for an active pharmaceutical ingredient. *Organic Process Research & Development*. **2013**, 17(3), 540-548.
10. Saganowska, P.; Wesolowski, M. DSC as a screening tool for rapid co-crystal detection in binary mixtures of benzodiazepines with co-formers. *Journal of Thermal Analysis and Calorimetry*, **2018,** 133, 785–795.
11. Harris, R.K. Application of solid-state NMR to pharmaceutical polymorphism and related matters. *J. Pharm. Pharmacol*. **2007**, 59, 225–239.
12. Vogt, F.G.; Clawson, J.S.; Strohmeier, M.; Edwards, A.J.; Pham, T.N.; Watsom, S.A. Solid-State NMR analysis of organic cocrystals and complexes. *Cryst. Growth Des.* **2009**, 9, 921–937.
13. An, J.H.; Lim, C.; Ryu, H.C.; Kim, J.S.; Kim, H.M.; Kiyonga, A.N.; Park, M.; Suh, Y.G.; Park, G,H.; Jung, K. Structural Characterization of Febuxostat/L-Pyroglutamic Acid Cocrystal Using Solid-State 13C-NMR and Investigational Study of Its Water Solubility. *Crystals,* **2017**, 7, 365.
14. Brackett, J.M.; Jonaitis, D.T.; Lai, W.; Liu, J. H.; Parent, S.D.; Shen, J. Solid state forms of racemic ilaprazole. PCT WO/2008/083333, 10 July 2008.
15. Liu, J. H.; Brackett, J.M.; Jonaitis, D.T.; Lai, W.; Parent, S.D. Crystalline forms of solvated ilaprazole. PCT WO/2008/083341, 10 July 2008.
16. Kim, J.W.; Suh, K.H.; Choi, Y.J.; Kwon, D.G.; Chae, S.Y. Crystalline form of Ilaprazole sodium and its new process. K.R. patent 1020210014900 A1 02 February 2021.
17. Wang, S.; Zhang, D.; Wang, Y.; Liu, X.; Liu, Y.; Xu, L. Gradient high performance liquid chromatography method for simultaneous determination of ilaprazole and its related impurities in commercial tablets. *Asian Journal of Pharmaceutical Sciences*, **2015,** 10(2), 146-151.
18. Rathore, S.B.S.; Sharma, A.; Garg, A.; Sisodiya, S. Formulation and evaluation of enteric coated tablet of Ilaprazole. *International Current Pharmaceutical Journal*, **2013**, 2(7), 126-130.
19. An, J.H.; Nam, S. Novel co-crystal of ilaprazole/xylitol. K.R. patent 102250509 B1 11 May 2021.
20. Geng, L.; Han, L.; Huang, L.; Wu, Z.; Wu, Z.; Qi, X. High anti-acid omeprazole lightweight capsule for gastro-enteric system acid-related disorders treatment. *J. Clin. Gastroenterol. Treat.* **2019**, 5, 1–11.
21. Kan, S.-L.; Lu, J.; Liu, J.-P.; Zhao, Y. Preparation and in vitro/in vivo evaluation of esomeprazole magnesium-modified release pellets. *Drug. Deliv*. **2016**, 23, 866–873.
22. He, W.; Yang, M.; Fan, J.H.; Feng, C.X.; Zhang, S.J.; Wang, J.X.; Guan, P.P.; Wu, W. Influences of sodium carbonate on physicochemical properties of lansoprazole in designed multiple coating pellets. *AAPS Pharm. Sci.Tech,* **2010**, 11, 1287–1293.
23. Wu, C.; Sun, L.; Sun, J.; Yang, Y.; Ren, C.; Ai, X.; Lian, H.; He, Z. Profiling biopharmaceutical deciding properties of absorption of lansoprazole enteric-coated tablets using gastrointestinal simulation technology. *Int. J. Pharm.* **2013**, 453, 300–306.
24. Quercia, R.A.; Fan, C.; Liu, X.; Chow, M.S.S. Stability of omeprazole in an extemporaneously prepared oral liquid. *Am. J. Health-Syst. Pharm.* **1997**, 54, 1833–1836.
25. El-Badry, M.; Taha, E.I.; Alanazi, F.K.; Alsarra, I.A. Study of omeprazole stability in aqueous solution: Influence of cyclodextrins. *J. Drug Deliv. Sci. Technol.* **2009**, 19, 347–351.
26. Horst, J.H.; Cains, P.W.; Co-crystal Polymorphs from a Solvent-Mediated Transformation. *Cryst. Growth Des.* **2008**, 8(7), 2537-2542.
27. Srebro, J.; Brniak, W.; Mendyk, A. Formulation of Dosage Forms with Proton Pump Inhibitors: State of the Art, Challenges and Future Perspectives. *Pharmaceutics*, **2022**, 14, 2043.
28. Stahl, P.H.; Wermuth, C.G. *Handbook of Pharmaceutical Salt Properties, Selection, and Use*; Wiley-Vch: Weinheim, Germany, 2002; pp. 272–320.
29. Elbagerma, M.A.; Edwards, H.G.M.; Munshi, T.; Scowen, I.J. Identification of a new cocrystal of citric acid and paracetamol of pharmaceutical relevance. *CrystEngComm,* **2011**, 13, 1877–1884.

 doi:10.20944/preprints202401.0270.v1

30. Zhou, Z.; Tong, H.H.Y.; Li, L.; Shek, F.L.Y.; Lv, Y.; Zheng, Y.; Synthesis, characterization and thermal analysis of ursolic acid solid forms. *Cryst. Res. Technol*. **2015**, 50(7), 538–548.